Acta Cryst. (1981). B**37**, 2164–2170

Electron-Density Distribution in Crystals of Tetra-μ-acetato-dimolybdenum(*Mo–Mo*)

BY K. HINO AND Y. SAITO*

The Institute for Solid State Physics, The University of Tokyo, Roppongi-7, Minato-ku, Tokyo 106, *Japan*

AND M. BÉNARD

ER n° 139 du CNRS, Université Louis Pasteur, 4 rue Blaise Pascal, 67084 *Strasbourg, France*

(*Received* 13 *November* 1980; *accepted* 23 *April* 1981)

Abstract

The electron-density distribution in crystals of $Mo_2(CH_3CO_2)_4$ has been determined by single-crystal X-ray diffractometry at 293 K [crystal data: $Mo_2(C_2H_3O_2)_4$, space group $P\bar{1}$, $a = 8{\cdot}4084\ (6)$, $b = 5{\cdot}4857\ (4)$, $c = 7{\cdot}5138\ (5)$ Å, $\alpha = 84{\cdot}13\ (1)$, $\beta = 105{\cdot}17\ (1)$, $\gamma = 105{\cdot}99\ (1)°$, $Z = 1$, $V = 321{\cdot}4\ (1)$ Å^3, $D_x = 2{\cdot}21$ Mg m^{-3}, μ(Mo $K\alpha$) = 1·917 mm^{-1}, final $R = 0{\cdot}024$ for 5497 observed reflections]. In general terms, a section of the deformation-density map perpendicular to and through the midpoint of the Mo–Mo bond shows diffuse residual density surrounding the bond in the form of a torus, the maximum being $0{\cdot}2\ (1)$ e Å^{-3}. On both sides of the Mo–Mo bond, there are disc-shaped peaks of $0{\cdot}3\ (1)$ e Å^{-3}, each 0·42 Å from the Mo atom. The valence-electron populations of the atoms were refined and the net charges of Mo, O and C atoms were estimated to be $+1{\cdot}16\ (8)$, $-0{\cdot}29\ (4)$ and $+0{\cdot}00\ (4)$ respectively. These and other features of the deformation density around the Mo atoms can be reasonably accounted for in terms of a classical picture of a quadruple Mo–Mo bond and also agree with the result of *ab initio* CI (configuration interaction) calculations for analogous $Mo_2(HCO_2)_4$.

Introduction

As part of a series of our studies on electron-density distribution in transition-metal compounds, the electron-density distribution in tetra-μ-acetato-dimolybdenum(II) was determined and compared with the result of *ab initio* CI calculations for analogous $Mo_2(HCO_2)_4$. Recent charge-density studies on binuclear species generally displayed a lack of features significantly different from zero in the region of the metal–metal bond on the deformation-density maps. In *trans*-$[(\pi\text{-}C_5H_5)Fe(CO)_2]_2$, a complete lack of residual densities was observed along the Fe–Fe line (Mitschler, Rees & Lehmann, 1978) in accordance with the absence of a direct metal–metal bond deduced from *ab initio* calculations (Bénard, 1978*b*, 1979*a*). However, the residual densities between the metal atoms were not really more significant in a compound for which a metal–metal bond obviously exists, namely $Mn_2(CO)_{10}$ (Rees, unpublished). On the other hand, in $(\eta^5\text{-}C_5H_5Ni)_2C_2H_2$ two substantial maxima appeared between the Ni nuclei along the bond at about 0·5 Å from the metal nucleus (Wang & Coppens, 1976). However, this result, obtained on a noncentrosymmetric complex, appears controversial since calculations of *ab initio* (Bénard, 1978*b*) and LCAO Hartree–Fock–Slater (Ros, unpublished) types both display similar density maps which are topologically different from the experimental map in the metal–metal region. More specifically the computed density maps do not show any significant accumulation region between the metal atoms. Recently, the electron-density distribution of $Cr_2(CH_3CO_2)_4.2H_2O$ was obtained and compared with the distribution computed from an *ab initio* wavefunction of $Cr_2(HCO_2)_4$ (Bénard, Coppens, De Lucia & Stevens, 1980). Even though the bonding in this compound is described in terms of a metal–metal quadruple bond (Cotton, 1975), weakened by a contribution from antibonding orbitals (Bénard, 1978*a*), the observed accumulation regions are neither high nor sharp, but large, diffuse and shallow, extending over the whole region of π and δ bonding.

This last study will provide a very useful comparison with the present work, performed on a complex which could be expected to be very similar to $Cr_2(CH_3CO_2)_4.2H_2O$ (same ligand, same electronic environment of the metal, same type of bonding expected), but which displays surprising differences that were never completely rationalized: difference of sensitivity of the metal–metal bond length to physical or chemical perturbations (Cotton, Extine & Gage, 1978; Cotton, Extine & Rice, 1978), difference in the strength of the quadruple bond and in the weight of the

* Present address: Department of Chemistry, Faculty of Science and Technology, Keio University, 3-14-1, Hiyoshi, Kohoku-ku, Yokohama 223, Japan.

0567-7408/81/122164-07$01.00

antibonding orbitals in the expansion of the wavefunction (Bénard, 1978*a*, 1979*b*). The study of the charge densities in the region of the Mo–Mo bond of the title compound may provide some additional information on these pending problems. After inspection of a number of known crystal structures of binuclear complexes, this compound was selected for the following reasons: (1) Of the Mo^{II}, W^{II} and Re^{III} complexes, the Mo complex has a small linear absorption coefficient for Mo $K\alpha$ radiation. (2) The compound is stable in dry air and also under X-irradiation. (3) The structure does not exhibit structural disorder. (4) The structure is simple: $P\bar{1}$, $Z = 1$, hence there are only a small number of parameters to be determined. The structure of this compound, previously reported in part by Lawton & Mason (1965), was redetermined by using more extensive data collected by diffractometry (Cotton, Mester & Webb, 1974).

Experimental

Single crystals were grown by vacuum sublimation at *ca* 573 K. A needle-shaped crystal was cut and shaped into a sphere. Cell dimensions were derived by least squares from the setting angles of 67 reflections ($40 \le 2\theta \le 42°$).

Intensity data were collected on a four-circle diffractometer equipped with a graphite monochromator, using Mo $K\alpha$ radiation. The experimental conditions are given in Table 1. The intensities were corrected for Lorentz and polarization effects. An absorption correction was also applied with the assumption of a spherical shape ($\mu r = 0{\cdot}52$) (Dwiggins, 1975).

Refinement

The refinement was carried out with the full-matrix least-squares program *RADIEL* (Coppens, Guru Row, Leung, Stevens, Becker & Yang, 1979). The function minimized was $R_w(F) = [\sum w(|F_o| - |F_c|)^2 / \sum w|F_o|^2]^{1/2}$, where the weight was defined by $w = 1/[\sigma(|F_o|)]^2$. The positional parameters for non-H atoms reported by Cotton *et al.* (1974) were used as a starting set. [Unfortunately, there is a typographical error in the reported parameters: the sign of the y parameter of C(3) should be minus, not plus.] After several cycles of least squares with anisotropic thermal parameters, the difference synthesis revealed the positions of all the H atoms in the methyl groups. They were then included in the refinement with isotropic thermal parameters. During the refinement it was apparent that some of the lower-order reflections are affected by extinction. An isotropic extinction correction was made (Zachariasen, 1967). The smallest extinction factor (F_o^2/F_c^2) was 0·55 for 100. The final correction factors for extinction effects, less than 0·90, are listed in Table 2.* An attempt to include anisotropic extinction coefficients failed. The valence-electron populations, the valence-form factor for Mo and the isotropic extinction parameters were included in the final refinement cycles. The atomic form factor for Mo was calculated by Dr Wakoh from the Hartree–Fock wavefunction of Mann (1967). The atomic form factors for O and C were taken from Fukamachi's (1971) table. For H atoms the form factors were taken from Stewart, Davidson & Simpson (1965). The anomalous-scattering terms for Mo, O and C were taken from *International Tables for X-ray Crystallography* (1974). The valence electrons whose populations and form factor were refined were chosen as listed in Table 5. The parameters converged to their self-consistent values after repetition of the following

* See deposition footnote.

Table 1. *Experimental conditions*

Crystal specimen	A sphere of 0·54 mm in diameter
Radiation	Mo $K\alpha$ ($\lambda = 0{\cdot}71069$ Å)
Monochromator	Graphite plate
Scan mode	θ–2θ continuous scan
Scan rate	2° min^{-1} in θ ($2\theta \le 80°$)
	1° min^{-1} in θ ($2\theta > 80°$)
Scan width	$1{\cdot}5° + 1{\cdot}0° \tan\theta$
Maximum number of repetitions	4 ($2\theta \le 60°$)
	6 ($60 < 2\theta \le 80°$)
	4 ($2\theta > 80°$)
Condition to terminate repetition	$\sigma(\|F\|)/\|F\| \le 0{\cdot}005$
$2\theta_{max}[(\sin\theta/\lambda)_{max}]$	97° (1·05 Å^{-1})
Number of observed unique reflections	5497

Table 3. *Positional parameters and equivalent isotropic thermal parameters (for* Mo $\times 10^5$; *for other non-*H *atoms* $\times 10^4$; *for* H $\times 10^3$) *with e.s.d.'s in parentheses*

$$U_{eq} = \tfrac{1}{3}\sum_i \sum_j U_{ij}\, a_i^* a_j^* \mathbf{a}_i.\mathbf{a}_j.$$

	x	y	z	U_{eq} (Å^2)
Mo	4399 (1)	16725 (2)	7315 (1)	2320 (3)
O(1)	−1754 (2)	807 (2)	1772 (2)	333 (4)
O(2)	−763 (2)	3647 (2)	−1610 (1)	301 (3)
O(3)	2695 (2)	2678 (2)	−214 (2)	347 (4)
O(4)	1687 (2)	−76 (2)	3131 (2)	323 (3)
C(1)	−2864 (2)	−1268 (3)	1296 (2)	335 (5)
C(2)	−1553 (2)	2427 (2)	−3076 (2)	292 (4)
C(3)	−4424 (3)	−1970 (6)	2046 (4)	505 (10)
C(4)	−2323 (3)	3803 (4)	−4754 (2)	419 (7)
H(1)	−401 (3)	−221 (5)	341 (4)	63 (7)
H(2)	−507 (3)	−349 (5)	154 (4)	51 (7)
H(3)	−496 (3)	−72 (5)	174 (4)	53 (7)
H(4)	−212 (3)	332 (5)	−587 (3)	41 (6)
H(5)	−184 (3)	561 (5)	−477 (4)	54 (7)
H(6)	−340 (3)	351 (5)	−493 (4)	56 (7)

three steps. First, the positional and thermal parameters for non-H atoms were determined from high-order reflections with $\sin\theta/\lambda \geq 0{\cdot}5$ Å^{-1}, because they are expected to show less bias from valence-density distributions. Secondly, a scale factor, an isotropic extinction parameter and the parameters of the H atoms were refined on the basis of all the observed reflections. Thirdly, the valence-electron populations and the valence form factor for Mo were refined using all the reflections. It is much more preferable to carry out the refinement including the complete set of structural parameters so as to obtain a more definitive result. However, correlation between parameters prevented us from carrying out such a procedure. Thus, neglect of the parameter interactions may have led to an underestimate of the errors. Nevertheless, the result obtained in this way always gives a plausible result, at least qualitatively (*e.g.* Ohba, Toriumi, Sato & Saito, 1978). The final discrepancy indices were $R(F) = \sum||F_o| - |F_c||/\sum|F_o| = 0{\cdot}024$ and $R_w(F) = 0{\cdot}029$ for 5497 observed reflections. In the last cycle of the refinement almost all the parameter shifts for non-H atoms were less than one tenth of the corresponding standard deviations. The final parameters are given in Table 3,* and fall mostly within the ranges listed in the previous paper (Cotton *et al.*, 1974). Fig. 1 shows an *ORTEP* drawing of the molecule (Johnson, 1965). The mean bond lengths and angles are listed in Table 4. The observed Mo–Mo distance of 2·0885 (5) Å is considerably shorter than that in metallic Mo of 2·725 Å, indicating a strong Mo–Mo interaction. The result of the charge refinement is given in Table 5. The central Mo atom is partly neutralized to about half its formal charge by donation of electrons from the ligating O atoms. This is in accordance with Pauling's electroneutrality rule (Pauling, 1960). In the last column of Table 5 the effective charges for $Mo_2(HCO_2)_4$ calculated from the Mulliken population analysis are given for comparison.

Two kinds of deformation density were calculated in which the calculated densities differed slightly. In the first one, hereafter designated as D_1, the subtracted density was calculated on the basis of a spherical atom with effective charges refined by electron-population analysis. Since the apparent contraction of the electron cloud around the metal atom was taken into account [$\kappa = 1{\cdot}092$ (4)], the resulting deformation density was expected to present the asphericity of electron redistribution clearly and to emphasize the chemical significance of the deformation density better. On the other hand, the residual density along the Mo–Mo bond may be overestimated, in view of the effective charge of Mo [+1·16 (6)]. In the second synthesis, hereafter designated as D_0, the calculated density was based on the neutral atoms averaged spherically in the ground state. In this calculation, the contraction of the charge density around the Mo atom was not taken into account and the scale factor was not adjusted. Then both deformation densities were averaged by assuming D_{4h} symmetry (Rees, 1976). The standard deviation of the observed electron density was estimated to be 0·08 e Å^{-3} at the general position (Stevens & Coppens, 1976). Fig. 2 shows the experimental deformation density. The calculations were carried out on a FACOM 230-48 computer at the Institute for Solid State Physics. Some calculations were performed on a Hitac 8800/8700 computer at the Computer Center of the University of Tokyo.

Table 4. *Averaged interatomic distances* (Å) *and bond angles* (°) *within the complex molecule*

D_{4h} symmetry was assumed. Values in parentheses are mean errors.

Mo–Mo	2·0885 (5)	C–O	1·272 (5)
Mo–O	2·118 (2)	C–C	1·496 (5)
Mo–Mo–O	91·8 (1)	O–C–O	121·8 (5)

Table 5. *Refinement of valence-electron populations*

	Core	Valence	Charge	Theoretical charge for $Mo_2(HCO_2)_4$
Mo	Kr	$(4s)^2(4p)^6(4d)^4$	+1·16 (8)	+1·21
O	He	$(2s)^2(2p)^6$	−0·29 (4)	−0·79
C	He	$(2s)^2(2p)^4$	0·00 (4)	+0·78

Valence form factor for Mo [defined by $f(s/\kappa)$] = 1·092 (4).

* A list of observed and calculated structure amplitudes, anisotropic thermal parameters and Table 2 have been deposited with the British Library Lending Division as Supplementary Publication No. SUP 36103 (36 pp.). Copies may be obtained through The Executive Secretary, International Union of Crystallography, 5 Abbey Square, Chester CH1 2HU, England.

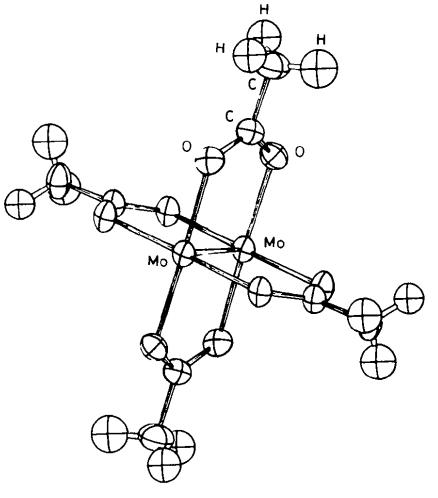

Fig. 1. An *ORTEP* drawing of the molecule. Ellipsoids of 50% probability are used for all the atoms (Johnson, 1965).

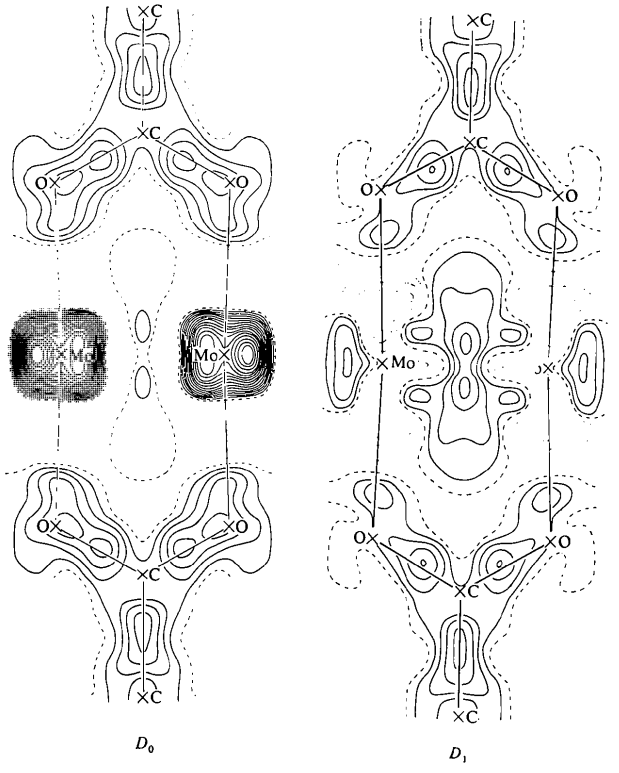

(*a*)

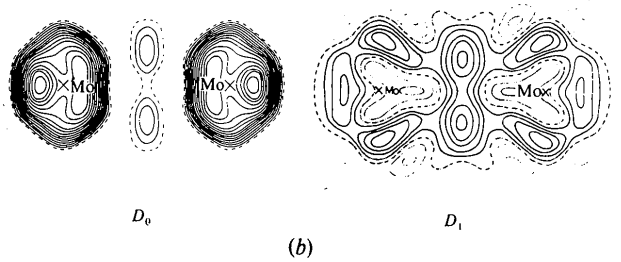

(*b*)

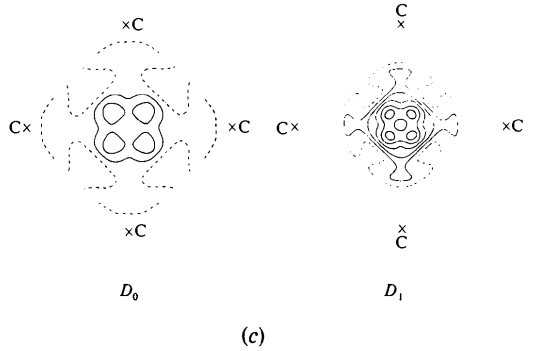

(*c*)

Fig. 2. Experimental deformation density of $Mo_2(CH_3CO_2)_4$. D_0 refers to the neutral atoms and D_1 refers to the charged atoms. (*a*) A section through the Mo–Mo bond and two acetate groups. (*b*) A section through the Mo–Mo bond and bisecting the two planes of the adjacent acetate groups. (*c*) A section through the midpoint of the Mo–Mo bond and perpendicular to it.

Molecular-orbital calculations

The theoretical density maps were obtained from *ab initio* LCAO–MO–SCF calculations on $Mo_2(HCO_2)_4$ carried out with the *ASTERIX* system of programs (Bénard, Dedieu, Demuynck, Rohmer, Strich & Veillard, unpublished; Bénard, 1976; Bénard & Barry, 1979). The Gaussian basis sets were (13, 9, 7) for Mo, (8, 4) for the first row atoms and (4) for H, contracted to a minimum basis set for inner shells and for the 4*s* and 5*p* shells of the Mo atoms, but a split set for the valence shells. The Mo–Mo distance was taken equal to 2·093 Å. The symmetry-adapted RHF closed-shell configuration which represents the one determinant ground state of the system (SCF configuration) displays four separate metal–metal bonds. One of these bonds is of σ type and involves the d_{z^2} orbitals of the Mo atoms (the *z* axis being collinear with the Mo–Mo line and the two Mo–O bonds being taken as *x* and *y* axes respectively). Two equivalent π bonds are obtained from the degenerate pairs of d_{xz} and d_{yz} orbitals. Finally, a weak δ bond appears from lateral overlap of the metal d_{xy} orbital. This SCF ground state, sometimes referred to as the $\sigma^2\pi^4\delta^2$ configuration, corresponds to the classical picture of the quadruple bond proposed by Cotton for the binuclear complexes involving metal atoms with an electronic configuration d^4. This configuration has an energy of −8685·188 a.u. (1 a.u. ≡ 27·190 eV). However, it has been shown that a limited expansion can significantly improve the energy, and, consequently, the description of the system (Bénard, 1978*a*). This CI expansion includes the ground state $\sigma^2\pi^4\delta^2$ as the leading term. This configuration interacts either directly or indirectly with the set of 15 configurations corresponding to one or several excitations of the type $a^2 \rightarrow a^{*2}$, where *a* denotes one of the four σ, π, $\bar{\pi}$, δ bonding orbitals (Bénard & Veillard, 1977; Bénard, 1978*a*). The effect of this CI develop-

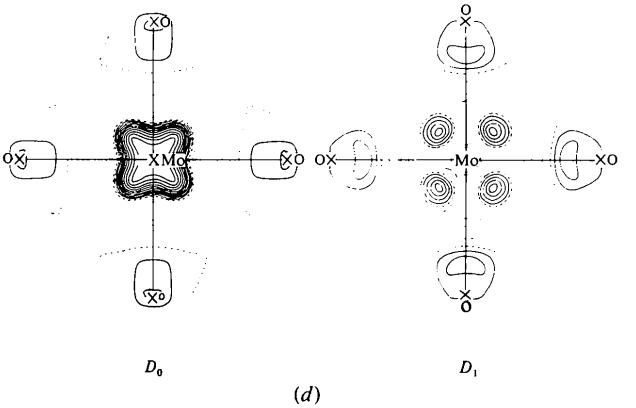

(*d*)

Fig. 2 (*cont.*) (*d*) A section through the plane formed by the Mo and the four ligating O atoms. Contours are drawn at intervals of 0·1 e Å^{-3}. Negative contours are dotted, zero contours being chain-dotted.

ment corresponds to an introduction in the wavefunction of contributions from the metal–metal antibonding orbitals, thus weakening the original quadruple bond and lowering the formal bond order. Even though this effect is much less drastic than for similar complexes of Cr (for which the CI expansion modifies the nature of the ground state), it is far from negligible. This can be seen from the energy associated with the CI expansion: −8685·441 a.u., lower than the SCF energy by as much as 0·253 a.u. and by the weight of the leading $\sigma^2\pi^4\delta^2$ configuration which is only 66%.*

The computed deformation-density distribution is defined as the function

$$\Delta\rho = \rho_{mol} - \sum \rho_{atom}$$

where ρ_{mol} represents the density obtained from the molecular wavefunction. The quantity ρ_{atom} corresponds to the density of a given atom of the system, considered isolated, neutral and spherically averaged, and located at its geometrical position in the molecule. This density is computed for the experimental ground state of the atom, with the same basis set as the one used for the molecular calculation. The summation $\sum \rho_{atom}$ is performed over all the atoms of the system. Four sections of the computed density distribution have been drawn in planes the locations of which are described in Fig. 3.

Results and discussion

It is to be noted that what is actually observed is not the charge distribution in an isolated molecule but that of a molecule in a crystal lattice. D_0 and D_1 remain convoluted with the atomic thermal motion (see Fig. 1). Accordingly, comparison of the observed and calculated residual density maps should be made with caution.

The theoretical deformation-density distribution (Fig. 3) has been computed with reference to the electron density of the 'promolecule' (Hirshfeld & Rzotkiewicz, 1974), that is, a superposition of neutral, spherically averaged atoms in their ground state. Thus comparison will be made mainly with the D_0 experimental distribution.

The general features of D_1 and D_0 can be qualitatively accounted for by the classical model of a quadruple bond. D_1 and D_0 are similar except in the vicinity of the Mo atom. In D_0 the peak at the center of the Mo–Mo bond reduced its height to about a half that of D_1. The piling up of the electron density is still significant in spite of the thermal-motion effect. A large difference between D_1 and D_0 occurs around the Mo

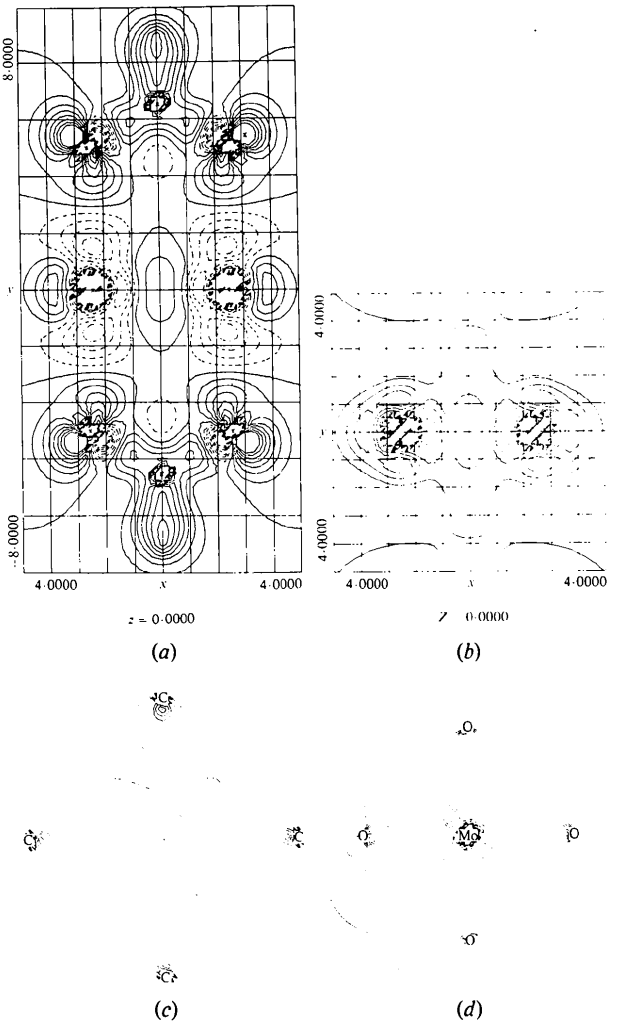

Fig. 3. Theoretical deformation density of $Mo_2(HCO_2)_4$. Sections as in Fig. 2. Contour interval 0·1 e Å^{-3}; CI D(Mo–Mo) = 2·093 Å.

atom. In D_0 a positive density, 1·5 e Å^{-3}, remains at the Mo nucleus and is surrounded by a spherical negative-density region (−0·6 e Å^{-3}) at 0·7 Å from the Mo nucleus. This difference arises from the neglect of κ on calculating D_0. The determined κ value of 1·092 (4) apparently indicates the contraction of electron density around the Mo atom; however, its physical interpretation is not so straightforward for several reasons: (*a*) The effect appears to be very important, since the peak reaches the unusual height of 1·5 e Å^{-3} even though the corresponding distribution accounts for the important thermal smearing at room temperature. However, no such accumulation had been recorded around the metal atoms at 90 K for $Cr_2(CH_3CO_2)_4.2H_2O$ (Bénard *et al.*, 1980). Such a steep density gradient is hardly compatible with the diffuse character of metal valence orbitals, which favors large accumulation zones of low density

* For $Cr_2(HCO_2)_4$ with experimental geometry, these quantities were respectively 0·684 a.u. and 18%.

gradient rather than sharp peaks in limited regions. (*b*) The existence of electron-deficient regions, around each Mo atom, at 0·7 Å from the metal nuclei, can be accounted for without requiring a drastic and isotropic contraction of valence orbitals (see discussion below). (*c*) The contraction of the metal valence orbitals is not supposed to be completely isotropic. In fact, the computed distributions for both Cr and Mo tetracarboxylates display an expansion of the d_{z^2} orbital associated with a contraction of the d_{xy} orbital. No clear intra-orbital charge transfer has been noticed for the π-bonding orbitals, d_{xz} and d_{yz}. These effects are significant, but they never induce peaks or troughs larger than 0·5 e Å^{-3} in the computed distribution. Consistent with the more diffuse character of valence orbitals in Mo, the effect of intra-orbital charge transfer on the theoretical maps is smoother for $Mo_2(HCO_2)_4$ than for $Cr_2(HCO_2)_4$.

Therefore, the presence of these large spherical accumulation zones around the metal atoms does not appear to be chemically significant. They are possibly artefacts related to the scale factor. This suggestion is made plausible by the high sensitivity of electron density near heavy atoms to a small variation of the scale factor (Rees, 1976, 1977, 1978). It is also possible that the effect of thermal diffuse scattering is unconsciously corrected by κ refinement, which was not considered in deriving $|F_o|$'s (De With, Harkema & Feil, 1976). Possibly the form factor for Mo is not adequate.

The other features of the experimental D_0 distribution can be readily correlated with the computed maps and with similar characters observed for $Cr_2(CH_3CO_2)_4.2H_2O$. The existence of a region of electron deficiency around Mo atoms has already been mentioned. These negative density regions are approximately spherical, but much deeper in the direction of the x and y axes. Another, less important minimum is observed along the z axis. The regions of electron deficiency along the x and y axes are obviously associated with the important depopulation of the $d_{x^2-y^2}$ orbital in the molecule with respect to the spherically averaged atomic orbital. The Mulliken population analysis of the computed wavefunction indicates that in terms of six d orbitals,* the population of orbitals $3d_{x^2} + 4d_{x^2}$, identical to that of $3d_{y^2} + 4d_{y^2}$, is 1·608 electrons, instead of 2 electrons in the spherical atom. However, there is a small increase of the overall population of the d_{z^2} orbital (2·087 electrons instead of 2). However, as for the tetracarboxylate of Cr, the electron population clearly moves towards the external part of the d_{z^2} orbital, thus generating along the z axis an electron-deficient zone at 0·5 Å from the metal atom and then a positive region around the center of symmetry of the system.

Even though the existence of negative regions centered along the x, y and z axes has been explained above, it is interesting to note that the metal atoms are surrounded, from approximately 0·5 to 1 Å, by a continuous electron-deficient environment, a character which is frequently encountered in transition-metal complexes (Mitschler *et al.*, 1978; Rees, 1976; Johansen, 1976). This has to be correlated with the important depopulation of the external s orbital, with respect to the neutral atom. This orbital is extremely diffuse and its depopulation produces a shallow trough at a relatively large distance from the nucleus. Therefore the accumulation regions associated with highly populated d orbitals often appear as isolated islands in a large and shallow negative environment. Since depopulation of the external s orbital of the metal is a fairly general and quantitatively important phenomenon in transition-metal complexes, its possible implications for deformation-density distributions must be considered in detail. More specifically, it might contribute to a significant reduction of the peak height at the center of a metal–metal bond. Concerning the present work, this interpretation is in agreement with the enhancement of the central accumulation region observed in the D_1 distribution for which the depopulation of the external s orbital has already been accounted in the contribution of the spherical atom. Similarly, in the theoretical distribution obtained for $Mn_2(CO)_{10}$, the small accumulation region between the Mn atoms is somewhat enhanced when the density difference is performed with respect to two $Mn(CO)_5$ fragments, in which the depopulation effect of the external s orbital is already introduced (Heijser, Baerends & Ros, 1980). This could provide a solution to the puzzling problems of rationalizing the absence of significant residues along a metal–metal bond (Bénard *et al.*, 1980).

In the regions of σ and π bonding, both experimental (D_0) and computed (CI) distributions display a large and diffuse accumulation region culminating between 0·1 and 0·2 e Å^{-3}. However, the two distributions present in this region a topological difference similar to what was observed for Cr tetracarboxylates. In the computed distribution (Fig. 3*a*) there is only one peak, located at the center of symmetry of the system. In the experimental distribution D_0 (Fig. 2*a*), even though the center of symmetry is slightly positive, contrary to the case of $Cr_2(CH_3CO_2)_4.2H_2O$, it corresponds to a saddle point separating two maxima symmetric with respect to the metal–metal axis. In the case of Cr tetracarboxylates, this discrepancy between computed and experimental distributions had been tentatively attributed to the effect of axial H_2O ligands in $Cr_2(CH_3CO_2)_4.2H_2O$, since these ligands were not taken into account in the wavefunction (Bénard *et al.*, 1980). However, this argument is not valid for

* *i.e.* without performing the transformation of d_{x^2}, d_{y^2} and d_{z^2} into $d_{z^2-x^2-y^2}$ and $d_{x^2-y^2}$.

$Mo_2(CH_3CO_2)_4$ which displays neither axial coordination nor significant intermolecular interaction in the crystal.

Another characteristic of the computed density map might be of interest from the chemical viewpoint, in comparison with Cr tetracarboxylate. A significant charge accumulation (0·25 e $Å^{-3}$) is visible along the z axis on the external side of each Mo atom. This region is unfortunately hidden on the experimental D_0 distribution by the big spherical accumulation region discussed above. However, the D_1 distribution displays a similar positive residue (Fig. 2*a* and *b*). In contrast, no such feature had been detected for $Cr_2(HCO_2)_4$. This could be correlated with the difference in sensitivity to axial coordination of Cr and Mo tetracarboxylates, extensively documented by Cotton *et al.* These authors have demonstrated that tetracarboxylates of Cr are extremely sensitive to axial coordination. Most of them either are associated with axial ligands or display strong intermolecular interactions in axial positions (Cotton, Extine & Gage, 1978). On the other hand, tetracarboxylates of Mo are almost completely insensitive to axial coordination (Cotton, Extine & Rice, 1978). This could be correlated with a shielding effect due to the electron-rich region close to the Mo atom which protects the metal from the approach of a ligand in an axial position.

Finally, it is worth mentioning that, contrary to the case of $Cr_2(HCO_2)_4$, the introduction of configuration interaction did not yield any significant modification of the deformation-density distribution, relative to the quadruply bonding configuration obtained at the SCF level. This confirms that the electronic structure of $Mo_2(HCO_2)_4$ is much closer to the classical scheme of the quadruple bond than that of $Cr_2(HCO_2)_4$ (Bénard, 1978*a*).

References

BÉNARD, M. (1976). *J. Chim. Phys. Phys. Chim. Biol.* **73**(4), 413–414.

BÉNARD, M. (1978*a*). *J. Am. Chem. Soc.* **100**, 2354–2362.

BÉNARD, M. (1978*b*). *J. Am. Chem. Soc.* **100**, 7740–7742.

BÉNARD, M. (1979*a*). *Inorg. Chem.* **18**, 2782–2785.

BÉNARD, M. (1979*b*). *J. Chem. Phys.* **71**, 2546–2556.

BÉNARD, M. & BARRY, M. (1979). *Comput. Chem.* **3**, 121–125.

BÉNARD, M., COPPENS, P., DE LUCIA, M. L. & STEVENS, E. D. (1980). *Inorg. Chem.* **19**, 1924–1930.

BÉNARD, M. & VEILLARD, A. (1977). *Nouv. J. Chim.* **1**, 97–99.

COPPENS, P., GURU ROW, T. N., LEUNG, P., STEVENS, E. D., BECKER, P. J. & YANG, Y. W. (1979). *Acta Cryst.* A**35**, 63–72.

COTTON, F. A. (1975). *Chem. Soc. Rev.* **4**, 27–53.

COTTON, F. A., EXTINE, M. & GAGE, L. D. (1978). *Inorg. Chem.* **17**, 172–176.

COTTON, F. A., EXTINE, M. & RICE, G. W. (1978). *Inorg. Chem.* **17**, 176–186.

COTTON, F. A., MESTER, Z. C. & WEBB, T. R. (1974). *Acta Cryst.* B**30**, 2768–2772.

DE WITH, G., HARKEMA, S. & FEIL, D. (1976). *Acta Cryst.* B**32**, 3178–3184.

DWIGGINS, C. W. JR (1975). *Acta Cryst.* A**31**, 395–396.

FUKAMACHI, T. (1971). Tech. Rep. B12. Institute for Solid State Physics, Univ. of Tokyo.

HEIJSER, W., BAERENDS, E. J. & ROS, P. (1980). *J. Mol. Struct.* **63**, 109–120.

HIRSHFELD, F. L. & RZOTKIEWICZ, S. (1974). *Mol. Phys.* **27**, 1319–1343.

International Tables for X-ray Crystallography (1974). Vol. IV. Birmingham: Kynoch Press.

JOHANSEN, H. (1976). *Acta Cryst.* A**32**, 353–355.

JOHNSON, C. K. (1965). *ORTEP*. Report ORNL-3794. Oak Ridge National Laboratory, Tennessee.

LAWTON, D. & MASON, R. (1965). *J. Am. Chem. Soc.* **87**, 921–922.

MANN, J. B. (1967). *Atomic Structure Calculations* I. Report LA-3690. Los Alamos Scientific Laboratory of the Univ. of California.

MITSCHLER, A., REES, B. & LEHMANN, M. S. (1978). *J. Am. Chem. Soc.* **100**, 3390–3397.

OHBA, S., TORIUMI, K., SATO, S. & SAITO, Y. (1978). *Acta Cryst.* B**34**, 3535–3542.

PAULING, L. (1960). *The Nature of the Chemical Bond.* 3rd ed. Ithaca: Cornell Univ. Press.

REES, B. (1976). *Acta Cryst.* A**32**, 483–488.

REES, B. (1977). *Isr. J. Chem.* **16**, 180–185.

REES, B. (1978). *Acta Cryst.* A**34**, 254–256.

STEVENS, E. D. & COPPENS, P. (1976). *Acta Cryst.* A**32**, 915–917.

STEWART, R. F., DAVIDSON, E. R. & SIMPSON, W. T. (1965). *J. Chem. Phys.* **42**, 3175–3187.

WANG, Y. & COPPENS, P. (1976). *Inorg. Chem.* **15**, 1122–1127.

ZACHARIASEN, W. H. (1967). *Acta Cryst.* **23**, 558–564.